Materials Science and Technology

ISSN: 0267-0836 (Print) 1743-2847 (Online) Journal homepage: http://www.tandfonline.com/loi/ymst20

Artificial neural network analysis of preparation of nano α-Al_2O_3 powders by thermal decomposition of ammonium aluminium carbonate hydroxide

H. J. Zhang, X. J. Wang, Q. L. Jia & H. W. Sun

To cite this article: H. J. Zhang, X. J. Wang, Q. L. Jia & H. W. Sun (2007) Artificial neural network analysis of preparation of nano α-Al_2O_3 powders by thermal decomposition of ammonium aluminium carbonate hydroxide, Materials Science and Technology, 23:9, 1021-1026, DOI: 10.1179/174328407X161376

To link to this article: https://doi.org/10.1179/174328407X161376

Published online: 19 Jul 2013.

Artificial neural network analysis of preparation of nano α-Al_2O_3 powders by thermal decomposition of ammonium aluminium carbonate hydroxide

H. J. Zhang*[1], X. J. Wang[1], Q. L. Jia[1] and H. W. Sun[2]

Nano α-Al_2O_3 powders were prepared by thermal decomposition of ammonium aluminium carbonate hydroxide (AACH). The effects of α-Al_2O_3 crystal seeds, reactant concentration, content of active agent (PEG), annealing temperature and ZnF_2 addition on the preparation of nano α-Al_2O_3 powder were studied. The results showed that nano α-Al_2O_3 powder with apparent crystallite size $\sim$40 nm could be prepared, and the complete transformation temperature of α-Al_2O_3 could be reduced from 1250 to 1050°C as α-Al_2O_3 seeds and ZnF_2 were added. The prepared nano α-Al_2O_3 powders were characterised by X-ray diffraction (XRD), differential thermal analysis and thermogravimetric (TG-DTA) and scanning electron microscopy (SEM). A back propagation (BP) artificial neural network (ANN) has been used to establish models between the relative content of the nano α-Al_2O_3 powders and the preparation parameters. The results of checking experiments were in accordance with the calculated values.

Keywords: α-Al_2O_3, Nano powders, Ammonium aluminium carbonate hydroxide, Preparation, Back propagation, Artificial neural network

Introduction

It is shown that artificial neural network (ANN) is a powerful modelling tool to identify complex relationships from input–output data in the existing literatures.[1–8] In the last decade, ANN technique has found widespread popularity among analytical chemists for solving chemicals problem for its following unique attributes:

(i) non-linearity allows better fit to the data
(ii) noise insensitivity provides accurate prediction in the presence of uncertain data and measurement errors
(iii) high parallelism implies fast processing and hardware failure tolerance,
(iv) learning and adaptivity allow the system to update (modify) its internal structure in response to changing environment
(v) generalisation enables application of the model to unlearned data.[9,10]

More accurate retention models can be obtained by using ANN technique than those by regression analysis and statistical testing.

Ultrafine alumina powder has received increasing attention owing to its wide applications in transparent and electronic ceramics, single crystals, abrasives and catalysts.[11] Some of non-conventional methods (different with the conventional Bayer procedure), such as hydrothermal synthesis,[12] microwave synthesis,[13] emulsion evaporation,[14] combustion synthesis[15] and precipitation from solution[16,17] were used for preparing the nanometre alumina powders. In this study, nano α-Al_2O_3 powders were prepared by thermal decomposition of ammonium aluminium carbonate hydroxide (AACH) which was synthesised by the homogeneous precipitation reaction of ammonium aluminium sulphate [$NH_4Al(SO_4)_2$] and ammonium hydrocarbonate (NH_4HCO_3). A back propagation (BP) ANN method was used for retention modelling between preparation parameters and the relative content of alumina in nano α-Al_2O_3 powders.

Experimental

The starting materials used in present paper were analytical reagent grade ammonium aluminium sulphate [$NH_4Al(SO_4)_2$], ammonium hydrocarbonate (NH_4HCO_3), ammonia solution, α-Al_2O_3 powders (used as crystal seeds, mean size 0·5 μm), ZnF_2 (mean size 44 μm, CP) and polypropylene glycol (PEG, mean molecular weight 950–1050, CP).

A stoichiometric amounts of $NH_4Al(SO_4)_2$ and NH_4HCO_3 were dissolved in distilled water respectively, then α-Al_2O_3 crystal seeds/ZnF_2/PEG (1, 3 and 5 wt-% relative to the final Al_2O_3 powders) were evenly dispersed in NH_4HCO_3 aqueous solution. The

[1]High Temperature Ceramics Institute, Zhengzhou University, Zhengzhou 450052, China
[2]Key Laboratory of Materials Physics, Ministry of Education, Zhengzhou University, Zhengzhou 450052, China

*Corresponding author, email zhjzdl@yahoo.com.cn

Published by Maney on behalf of the Institute
Received 25 August 2006; accepted 12 September 2006
DOI 10.1179/174328407X161376

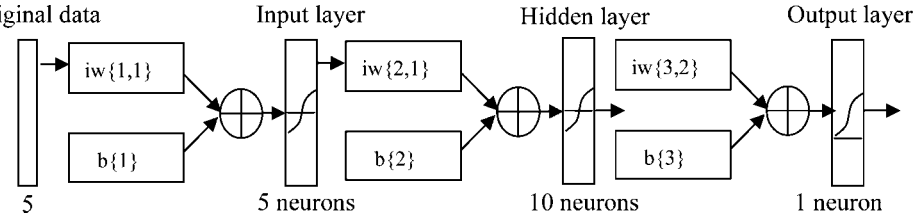

1 Illustration of three layered neural network with one input layer, one hidden layer and one output layer

$NH_4Al(SO_4)_2$ aqueous solution (0·2–0·4 mol L^{-1}) was dropwisely added to the aqueous solution of NH_4HCO_3 (2 mol L^{-1}) at pH 9·0 and 40°C to get AACH. The speed of titration of $NH_4Al(SO_4)_2$ was ~15 mL min^{-1}. In order to let $NH_4Al(SO_4)_2$ react completely, the amount of NH_4HCO_3 was kept excess (30 wt-%). The precipitate reaction is as following

$$NH_4Al(SO_4)_2{\cdot}12H_2O + 4NH_4HCO_3 = NH_4Al(OH)_2CO_3 + 2(NH_4)2SO_4 + 3CO_2 + 13H_2O \quad (1)$$

The precipitate was then aged at 60°C for 18 h. The aged AACH powders were annealed at 950–1150°C for 2 h to get the nanosized α-Al_2O_3 powders. The decomposition reaction of the AACH is as following

$$NH_4Al(OH)_2CO_3 = Al_2O_3 + NH_3\uparrow + CO_2\uparrow + H_2O\uparrow \quad (2)$$

Differential thermal analysis coupled with thermogravimetric analysis of the precursor (AACH) was carried out on a NETZSCH STA-449C thermal analysis system with a rising temperature rate of 10 K min^{-1} in flowing air. The sample weight was 30 mg. The sample pot was alumina with a depth of 5 mm, and the reference material was alpha-alumina.

X-ray diffraction (XRD) patterns were recorded from 20 to 80° (2θ) with a step width of 0·02° using a Philips X'Pert PRO diffractometer with Cu K_α radiation. The apparent crystallite size of the final α-Al_2O_3 powders was determined using the Scherrer formula. The relative content of the prepared alumina (represented as RCA, and expressed in arbitrary units) in final product was estimated approximately by the following formula

$$P\% = A_i / \Sigma A_{ij} \quad (3)$$

where P% is the relative content of alumina, A_i is the absolute integral area of the strongest characteristic peaks of i composition (α, θ and γ-Al_2O_3), and ΣA_{ij} is the summation of the integral area of characteristic peak for all crystal phases in final product, (104) reflection (2θ is ~35·15°) of α-Al_2O_3, ($\bar{4}01$) reflection (2θ is ~31·51°) of θ-Al_2O_3, and (400) reflection (2θ is ~45·67°) of γ-Al_2O_3 were used for calculation.

The powder morphology was observed via scanning electron microscopy (Model JSM-5610LV, JEOL, JAPAN) and field emission scanning electron microscopy (FESEM) (Model JSM-6700F, JEOL, JAPAN, 15 kV). The powders sample was ultrasonically dispersed into water, and the resultant suspension was spread on the surface of a polished silicon plate. The samples were coated with a thin layer of platinum for conductivity before SEM and FESEM observation.

Artificial neural network approach

Back propagation learning algorithm was used in this study. This network has one input layer, one hidden layer and one output layer; the architecture of the ANN model is shown in Fig. 1. To train and test the neural networks, input data patterns and corresponding targets were required. In developing a ANN model, the available data set was divided into two sets, one to be used for training of the network (specimen No. 1 to 46 in Tables 1–5), and the remaining was used to verify the generalisation capability of the network (specimen No. 47–52 in Table 5). The mathematical background, the procedures for training and testing the ANN and account of its history can be found in the text by Haykin.[18] Input–output pairs are presented to the

Table 1 Effect of concentration of ammonium aluminium sulphate [$NH_4Al(SO_4)_2$] on preparation of Al_2O_3 powders*

Code no.	$NH_4Al(SO_4)_2$, mol L^{-1}	Annealing temperature, °C	Crystalline size, nm	Relative content of α-Al_2O_3, %
1	0·2	1150	49	22
2	0·3	1150	43	78
3	0·4	1150	37	81
4	0·2	1100	–	0
5	0·3	1100	–	0
6	0·4	1100	–	0

*No additive, crystal seeds and ZnF_2 added.

Table 2 Effect of amount of additive (PEG) on preparation of Al_2O_3 powders*

Code no.	PEG, wt-%	Annealing temperature, °C	Crystalline size, nm	Relative content of α-Al_2O_3, %
7	1	1150	36	69
8	3	1150	40	66
9	5	1150	55	51
10	1	1100	–	0
11	3	1100	–	0
12	5	1100	–	0

*[$NH_4Al(SO_4)_2$]=0·3 mol L^{-1}; no crystal seeds and ZnF_2 added.

network, and weights are adjusted to minimise the error between the network output and actual value. Once training is completed, predictions from a new set of data may be done using the already trained network. The ANN model is composed of five neurons in the input layer, one neuron in the output layer and ten neurons were used in hidden layer. The inputs neurons were concentration of $NH_4Al(SO_4)_2$ (NS), the amount of the PEG (PEG), the amount of alumina crystal seeds (Seed), the amount of ZnF_2 (ZF) and annealing temperature (T). One object output neurons were the relative content of α-Al_2O_3 in final product annealed at 950–1150°C.

The Neural Networks Toolbox of MATLAB 6·5 was used to form the ANN. The tan–sigmoid transfer function was used in the input layer and hidden layer, and log–sigmoid transfer function in the output layer. The BP network training function updates weight and bias values according to Levenberg–Marquardt optimisation.[19] Mean squared error (MSE) that determine network performance is formulated as follows

$$\mathrm{MSE}=\frac{1}{N}\sum_{\mathrm{i}=1}^{\mathrm{N}}(y_{\mathrm{i}}-y_{\mathrm{k}})^2 \tag{4}$$

where y_i is the predicted value of the ith pattern, y_k is the target value of the ith pattern and N is the number of pattern.

Table 3 Effect of amount of alumina crystal seeds on preparation of Al_2O_3 powders*

Code no.	Seeds, wt-%	Annealing temperature, °C	Crystalline size/nm	Relative content of α-Al_2O_3, %
13	1	1150	38	99
14	1	1100	37	98
15	1	1050	38	53
16	1	1000	–	0
17	1	950	–	0
18	3	1150	41	99
19	3	1100	40	99
20	3	1050	44	96
21	3	1000	40	75
22	3	950	42	77
23	5	1150	41	95
24	5	1100	40	88
25	5	1050	44	64
26	5	1000	40	63
27	5	950	42	73

*$[NH_4Al(SO_4)_2]$=0·3 mol L^{-1}; PEG 1 wt-%; no ZnF_2 added.

Table 4 Effect of amount of ZnF_2 on preparation of Al_2O_3 powders*

Code no.	ZnF_2, wt-%	Annealing temperature, °C	Crystalline size, nm	Relative content of α-Al_2O_3, %
28	1	1150	39	73
29	1	1100	39	78
30	1	1050	42	55
31	1	1000	40	51
32	1	950	–	0
33	3	1150	44	97
34	3	1100	40	94
35	3	1050	36	76
36	3	1000	33	81
37	3	950	–	0
38	5	1150	48	99
39	5	1100	43	97
40	5	1050	40	90
41	5	1000	50	66
42	5	950	–	0

*$[NH_4Al(SO_4)_2]$=0·3 mol L^{-1}; PEG 1 wt-%; no crystal seeds.

Table 5 Effect of addition of crystal seeds and ZnF_2 on preparation of Al_2O_3 powders*

Code no.	ZnF_2, wt-%	Annealing temperature, °C	Crystalline size, nm	Relative content of α-Al_2O_3, %
43	5	1000	45	81
44	5	950	43	85
45	3	1000	41	80
46	3	950	12	63
47	3	1150	47	97
48	3	1100	44	97
49	3	1050	43	90
50	5	1150	46	98
51	5	1100	38	93
52	5	1050	42	91

*$[NH_4Al(SO_4)_2]$=0·3 mol L^{-1}; PEG 1 wt-%; α-Al_2O_3 seeds 5 wt-%.

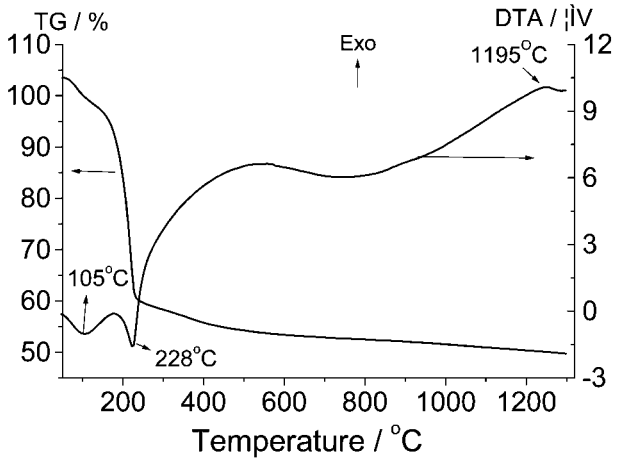

2 Differential thermal analysis and thermogravimetric curves of $NH_4Al(OH)_2CO_3$ by homogeneous precipitation reaction: [NH4Al(SO4)2]=0·3M; no PEG, crystal seeds and ZnF2 added

Results and discussion

The differential thermal analysis and thermogravimetric (TGDTA) curves of the dry AACH are shown in Fig. 2. The small endothermic peak at $\sim$150°C in the DTA trace accounted for $\sim$1% of the initial weight loss in TG can be assigned to the removal of absorbed moisture. The endothermic peak at 228°C in the DTA curves with $\sim$51% weight loss can be attributed to the decomposition of the AACH, after that there is almost no change in weight loss that can be attributed to the formation of a pure oxide system. No exothermic peak results from the transformation from amorphous alumina to γ-Al_2O_3 and θ-Al_2O_3 can be clearly observed in the DTA curves in 400–1000°C. The exothermic peak at 1195°C in the DTA curves may be due to the formation of α-Al_2O_3.

Tables 1–5 show the effects of the concentration of $NH_4Al(SO_4)_2$ (NS), the amount of the PEG (PEG), the amount of alumina crystal seeds (Seed), and the amount of ZnF_2 (ZF) on the relative content of α-Al_2O_3 (RCA) in the final powders at different annealing temperatures (T). From the results, it can be seen that:

(i) the relative content of α-Al_2O_3 in final powder increases with increasing concentration of ammonium aluminium sulphate; the crystalline size of the final α-Al_2O_3 decreases with increasing concentration of ammonium aluminium sulphate. The dried AACH precipitate annealed at 1150°C for 2 h, still gives strong θ-Al_2O_3 peak and amorphous background, because in this temperature transition alumina can not be completely converted to α-Al_2O_3. This is clearly illustrated in Fig. 3 showing the XRD patterns of specimen No. 2 and 5 fired at 1100–1150°C

(ii) suitable amount of the PEG will lower the crystalline size of the final α-Al_2O_3, comparing the results in Table 2 with Table 1, it indicates that the sample with 1 wt-%PEG addition possess the higher value of the relative content of α-Al_2O_3 and the smaller α-Al_2O_3 crystalline size

(iii) the presence of α-Al_2O_3 crystal seeds in AACH precipitate is favourable to the transformation from θ-Al_2O_3 to α-Al_2O_3 at lower temperature. Table 3 clearly indicates that the relative content of α-Al_2O_3 for the samples with crystal seeds added is much more than that of the samples without crystal seeds. The inceptive formation temperature of the samples with α-Al_2O_3 crystal seeds is $\sim$150°C lower than that of the samples without crystal seeds added. The dried AACH precipitate with 3 wt-% α-Al_2O_3 crystal seeds added, calcined over 1050°C for 2 h, can be near completely converted to α-Al_2O_3, but when calcined at 950–1000°C (as shown in Fig. 4), the XRD only shows weak diffraction peaks of α-Al_2O_3, θ-Al_2O_3 and amorphous background. The θ-Al_2O_3 XRD pattern is broad indicating the existence of fine crystallite. The effects of the seeds on the final α-Al_2O_3 can be explained on the basis that the crystal seeds act as substrates for heterogeneous nucleation.[20] The annealing temperature and the amount of the crystal seeds have a little effect on the crystallite size of the final α-Al_2O_3 powders, and its crystallite sizes is $\sim$40 nm, which is determined by the XRD line broadening technique

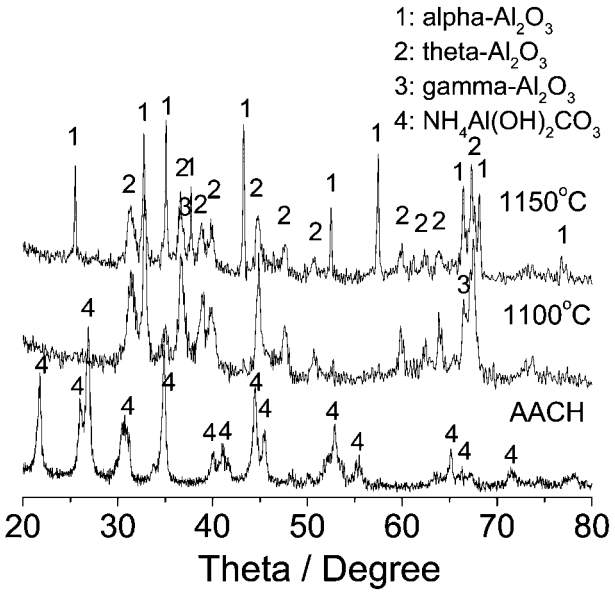

3 X-ray diffraction results of sample without crystal seeds annealed at 1100–1150°C (α-Al2O3: JCPDS 46-1212; θ-Al2O3: JCPDS 23-1009; γ-Al2O3: JCPDS 50-0741; NH4Al(OH)2CO3: JCPDS 76-1923)

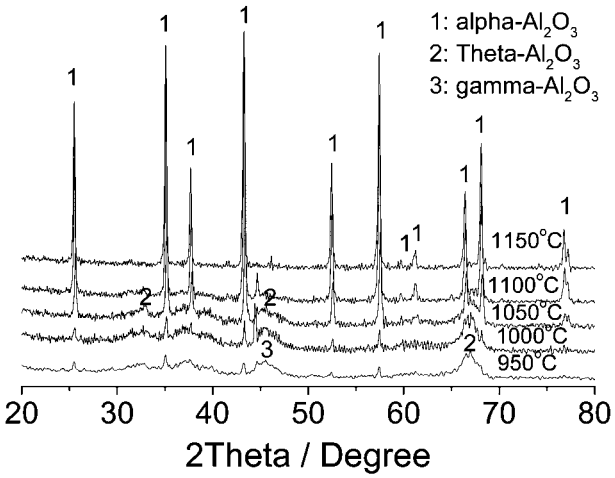

4 X-ray diffraction results of sample with 3 wt-% crystal seeds annealed at 950–1150°C

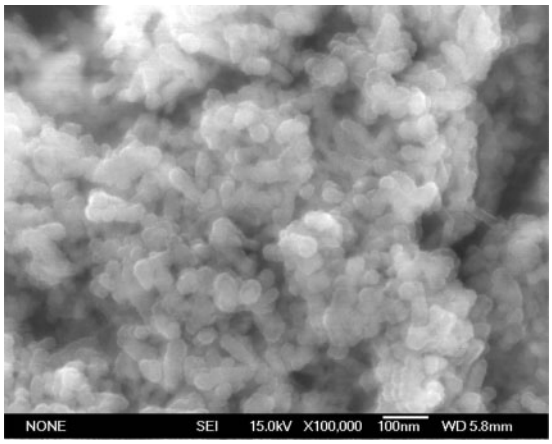

5 Image (FESEM) of α-Al_2O_3 annealed at 1050°C for 2 h

(iv) ZnF_2 additive has potential synergistic effects for reduction in the transformation temperature of α-Al_2O_3 (as shown in Table 4). It may be due to the formation of an intermediate compound, AlOF, which accelerates the mass transportation from transition alumina to α-Al_2O_3.[21] The amount of ZnF_2 has no significant effects on the crystal size of the final α-Al_2O_3. Table 5 indicates that the initial crystallisation temperature of the α-Al_2O_3 from the AACH precipitate simultaneously added with α-Al_2O_3 seeds and ZnF_2 was ~950°C (200°C lower than that of the pure AACH samples).

Figure 5 shows FESEM morphology of the α-Al_2O_3 powders prepared at 1050°C for 2 h, and it revealed that these α-Al_2O_3 particles possessed global structures with diameters about 30–50 nm, which coincides with the results of the Scherrer formula. However, the particle is congregated together which can be attributed to the high surface activity of the powders.

The aim of using the ANN model considered as a practical approach is to test the ability to predict the relative content of the final α-Al_2O_3. After 428 training cycles the level of error was satisfactory and further cycles had no significant effect on error reduction. This clearly illustrates in Fig. 6. During the training and testing/validation period, the maximum mean relative error was found to be 0·001%. This good predictive ability can be observed from Fig. 7, indicating that the

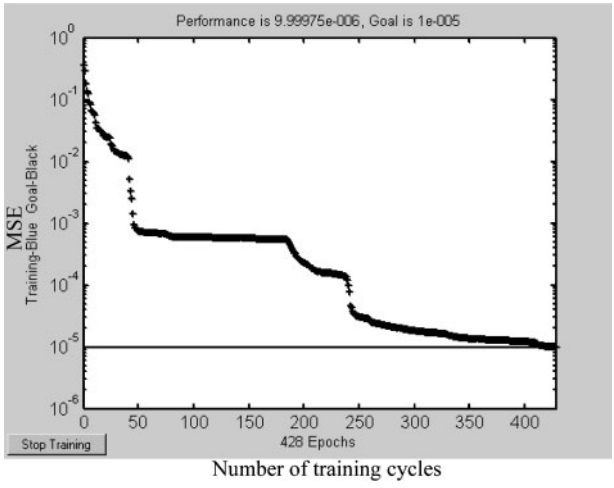

6 Performance of proposed neural network configuration

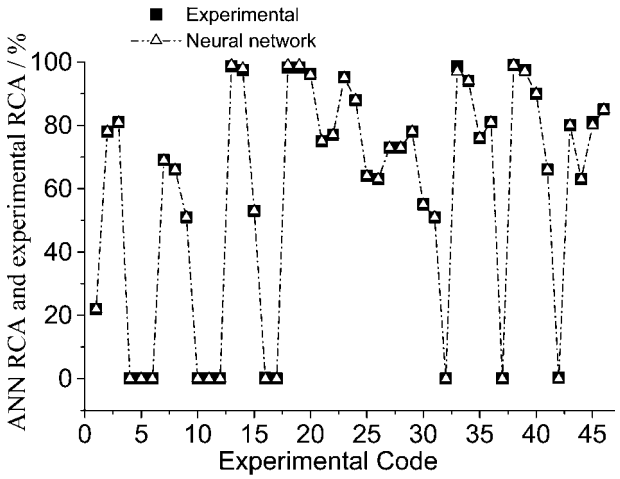

7 Correlation between experimental RCA (relative content of alumina in final product) and calculated RCA by ANN model: 10 neurons in hidden layer and 428th iteration in training

network was able to accurately learn the training data sets. Six experimental values are selected to verify the correctness of the ANN, a comparatively presentation of the error during testing by using trained network and experimental results is shown in Fig. 8. The relative errors in the testing period between predicted and measured values were found to be in the range 1–7%. The mean relative error during testing was found to be 3·4% in predicting the relative content of the final α-Al_2O_3. Predictive ability of the network was found to be satisfactory. The relationship between the calculated RCA and the experimental RCA can be expressed as following

$$y = iw\{3,2\}iw\{2,1\}$$
$$\tan\{iw\{1,1\}\tan(x + b\{1\}) + b\{2\}\} + b\{3\} \quad (5)$$

where y is the calculated RCA by ANN; x is the experimental RCA; iw{1,1}: weight to layer 1 from input; iw{2,1}: weight to layer; iw{3,2}: weight to layer; b{1}: bias to layer 1; b{2}: bias to layer 2; b{3}: bias to layer 3. The values of iw{1,1}, iw{2,1}, iw{3,2}, b{1}, b{2} and b{3} are showed in appendix.

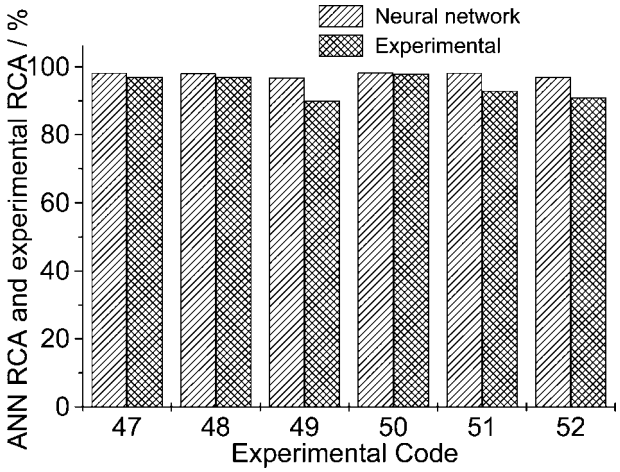

8 Comparison between outputs of network and testing results: 10 neurons in hidden layer and 428th iteration in training

Conclusions

Nanosized α-Al_2O_3 powders were prepared by thermal decomposition of ammonium aluminium carbonate hydroxide (AACH) using ammonium aluminium sulphate [$NH_4Al(SO_4)_2$], ammonium hydrocarbonate (NH_4HCO_3), etc. as starting materials. The addition of α-Al_2O_3 seeds and ZnF_2 additives could promote the formation of the final α-Al_2O_3 and lower its crystallisation temperature. The initial crystallisation temperature of the α-Al_2O_3 from the AACH precipitate with α-Al_2O_3 seeds and ZnF_2 added was $\sim$950°C (200°C lower than that of the pure AACH samples). The prepared nanosized α-Al_2O_3 particles possessed global structures with diameters about 30–50 nm.

A BP ANN with a 5–10–1 (number of input layer–hidden layer–output layer nodes) configuration was developed for predicting the relative content of α-Al_2O_3 (RCA) in final product prepared by the decomposition of AACH. The calculated results by ANN were $<$0·001% average relative error compared with those obtained experimentally.

Appendix

$$\begin{aligned}\mathrm{iw}\{1,1\} = [&2{\cdot}0591 - 0{\cdot}048869{\cdot}2{\cdot}8455{\cdot}0{\cdot}88971 - \\ &0{\cdot}62386; 9{\cdot}047{\cdot}3{\cdot}3847{\cdot}1{\cdot}4587 - 1{\cdot}233{\cdot}2{\cdot}7632; \\ &10{\cdot}2256{\cdot}7{\cdot}793{\cdot}0{\cdot}84291 - 0{\cdot}38746 - \\ &2{\cdot}6265; 12{\cdot}1552{\cdot}4{\cdot}0274 - 1{\cdot}8823{\cdot}0{\cdot}57511 - \\ &0{\cdot}38757; 9{\cdot}8745{\cdot}2{\cdot}4666{\cdot}0{\cdot}19952 - 0{\cdot}03991 - \\ &1{\cdot}103]\end{aligned} \quad (1)$$

$$\begin{aligned}\mathrm{iw}\{2,1\} = [&0{\cdot}20766 - 0{\cdot}30602 - 1{\cdot}5836 - 1{\cdot}7004 - \\ &0{\cdot}18291; 17{\cdot}5526 - 0{\cdot}29552 - 1{\cdot}1878{\cdot}3{\cdot}4021{\cdot}7{\cdot}1075; - \\ &7{\cdot}5995 - 0{\cdot}86315{\cdot}0{\cdot}43198 - 4{\cdot}2662{\cdot}0{\cdot}99596; 0{\cdot}89959 - \\ &7{\cdot}9702 - 4{\cdot}3258{\cdot}0{\cdot}94691{\cdot}1{\cdot}3585; 1{\cdot}1449 - 3{\cdot}9352 - \\ &1{\cdot}0794 - 1{\cdot}1151 - 0{\cdot}1431; 2{\cdot}0446 - 2{\cdot}6774 - 3{\cdot}104 - \\ &0{\cdot}53809 - 0{\cdot}11937; 1{\cdot}5736{\cdot}3{\cdot}7265{\cdot}5{\cdot}2679{\cdot}0{\cdot}79899{\cdot} \\ &1{\cdot}2114; 0{\cdot}76329{\cdot}1{\cdot}5397 - 0{\cdot}071681 - 4{\cdot}526 - 1{\cdot}6109; - \\ &1{\cdot}2706 - 0{\cdot}53044 - 0{\cdot}45698{\cdot}1{\cdot}463{\cdot}0{\cdot}41304; - \\ &12{\cdot}5501 - 5{\cdot}8655 - 1{\cdot}231 - 3{\cdot}1046{\cdot}2{\cdot}0493]\end{aligned} \quad (2)$$

$$\begin{aligned}\mathrm{iw}\{3,2\} = [&2{\cdot}9249 - 9{\cdot}1515 - 3{\cdot}73{\cdot}8{\cdot}4245{\cdot}1{\cdot}313 - \\ &0{\cdot}5776{\cdot}8{\cdot}3939{\cdot}1{\cdot}0782{\cdot}14{\cdot}8051 - 7{\cdot}0027]\end{aligned} \quad (3)$$

$$\mathrm{b}\{1\} = [0{\cdot}75021; -1{\cdot}2875; 0{\cdot}18907; 3{\cdot}6107; -1{\cdot}7953] \quad (4)$$

$$\begin{aligned}\mathrm{b}\{2\} = [&-2{\cdot}8142; 3{\cdot}5419; 0{\cdot}71865; -0{\cdot}34433; \\ &-0{\cdot}84256; -0{\cdot}8861; 0{\cdot}0034983; -0{\cdot}2523; -0{\cdot}3674; \\ &-2{\cdot}6089]\end{aligned} \quad (5)$$

$$\mathrm{b}\{3\} = [-1{\cdot}544] \quad (6)$$

References

1. S. A. Kalogirou, S. Panteliou and A. Dentsoras: *Solar Energy*, 1999, **65**, 335–342.
2. S. A. Kalogirou and M. Bojic: *Energy*, 2000, **25**, 479–491.
3. H. Bechtler, M. W. Browne, P. K. Bansal and V. Kecman: *Appl. Therm. Eng.*, 2001, **21**, 941–953.
4. J. Xu, H. Y. Ge, X. L. Zhou, J. L. Yan, Q. Chi and Z. P. Zhang: *J. Biomed. Informat.*, 2005, **38**, 417–421.
5. N. K. Bose and P. Liang (eds.): 'Neural network fundamentals with graphs, algorithms, and applications'; 1996, New York, McGraw-Hill Press.
6. W. G. Baxt: *Lancet*, 1995, **346**, 1135–1138.
7. K. Huang, F.-Q. Chen and D.-W. Lu: *Appl. Catal. A*, 2001, **219A**, 61–68.
8. D. M. Liu: *J. Mater. Sci. Lett.*, 1996, **15**, 419.
9. I. A. Basheer and M. Hajmeer: *J. Micro. Meth.*, 2000, **43**, 3–31.
10. D. Guo, Y. L. Wang, J. T. Xia, C. Nan and L. T. Li: *J. Eur. Ceram. Soc.*, 2002, **22**, 1867–1872.
11. C.-C. Ma, X.-X. Zhou, X. Xu and T. Zhu: *Mater. Chem. Phys.*, 2001, **72**, 374–379.
12. S. F. Tikhov, Y. V. Potapova, V. A. Sadykov, V. B. Fenelonov, I. V. Yudaev, O. B. Lapina, A. N. Salanov, V. I. Zaikovkii and G. S. Litvak: *Mater. Res. Innovat.*, 2005, **9**, (3), 69–71.
13. H. C. Park, Y. B. Lee, S. G. Lee, C. H. Lee, J. K. Kim and S. S. Park: *Ceram. Int.*, 2005, **31**, (2), 293–296.
14. Y. Sarikaya, I. Sevinc and M. Akinc: *Powder Technol.*, 2001, **116**, 109–114.
15. L. C. Pathak, T. B. Singh, S. Das, A. K. Verma and P. Ramachandrarao: *Mater. Lett.*, 2002, **57**, 380–385.
16. K. Morinaga, T. Torikai, K. Nakagawa and S. Fujino: *Acta Mater.*, 2000, **48**, 4735–4741.
17. Y. Q. Wu, Y.-F. Zhang, X.-X. Huang and J.-K. Guo: *Ceram. Int.*, 2001, **27**, 265–268.
18. S. Haykin: 'Neural networks, a comprehensive foundation'; 1994, New York, McMillian College Publishing Company.
19. M. T. Hagan, H. B. Demuth and M. Beale: 'Neural network design'; 1995, Boston, MA, PWS Publishing Company.
20. W. D. Kingery: 'Introduction to ceramics', 286; 1960, New York, London, John Wiley & Sons, Inc.
21. M. V. Swain: *Mater. Sci. Technol.*, 1994, **11**, 89.